SLAC-PUB-1230
(T-E)
April 1973

On Shadowing in Photoproduction and Inelastic Electron Scattering from Complex Nuclei [+]

by D. Schildknecht [++]
Stanford Linear Accelerator Center
Stanford University, Stanford, California 94305

+ Work supported in part by the U.S. Atomic Energy Commission

++ Permanent address and address after January 1st, 1973
Deutsches Elektronen-Synchrotron DESY, Hamburg, Germany

(Submitted to Nucl. Phys. B)

Abstract

The question of higher mass vector state contributions to shadowing in photo- and electroproduction is investigated quantitatively in a simple optical model approach. A large amount of shadowing comparable in magnitude to the one found in photoproduction is predicted also for inelastic electron or muon scattering a moderately large q^2 ($\lesssim$ 2 GeV^2/c^2) as soon as the energy of the virtual photon lies in the 100 GeV range. Comparison with the available inelastic electron scattering data below 17 GeV ($q^2 \lesssim 1.5$ GeV^2/c^2) shows that even the ρ^o,ω,Φ contribution to shadowing is larger than the experimentally observed shadow. Further experimental work establishing more clearly the transition from strong shadowing in photoproduction ($q^2 = 0$) to its vanishing at sufficiently high q^2 would be desirable to clarify the situation.

1. Introduction

As has been shown [1) +] recently, generalized vector dominance, i.e. supplementing the ρ^o,ω,ϕ contribution to the virtual forward Compton amplitude by more massive states as produced in e^+e^- annihilation at higher energies, provides a quantitative description of deep inelastic electron nucleon scattering. Although the transverse total virtual photon proton cross section $\sigma_T(W^2,q^2)$ in the large ω' region ($\omega'-1 \equiv W^2/q^2$, W virtual photon nucleon center of mass energy, $q^2 > 0$ spacelike, photon four momentum squared) within this framework is described essentially without an adjusted parameter, further tests of the model are of course desirable. Rather unambiguous tests can be obtained from more refined data on e^+e^- annihilation beyond the ρ^o,ω,Φ region in conjunction with photo- and electroproduction of higher mass photonlike states e.g. by coherent production from complex nuclei. However, as higher mass vector states may perhaps dominantly decay into many pions (as it seems to be the case for the ρ' [3)] , photo- and electroproduction experiments of still higher mass photonlike states may be difficult to realize, and one is asked to look for more indirect tests of generalized vector dominance (GVD).

As is well known [4-9)], measurements of the total absorption cross section for real or virtual spacelike photons from complex nuclei, $\sigma^{\gamma A}$, provide a significant test of the vector dominance sum rule [4,10)], which connects the transverse virtual forward Compton amplitude from nucleons $f^T_{\gamma\gamma}$ with the forward production amplitude $f^T_{\gamma V}$ for transverse vector mesons V by transverse virtual photons[++] and with the transverse vector meson forward scattering amplitude f^T_{VV} by

$$f^T_{\gamma\gamma} = \int_V \frac{\sqrt{\alpha\pi}}{\gamma_V} \frac{m_V^2}{(q^2+m_V^2)} f_{\gamma V} = \int_V \frac{\alpha\pi}{\gamma_V^2} \frac{m_V^4}{(q^2+m_V^2)^2} f^T_{VV}, \qquad (1)$$

where in GVD [1)] the sum $\int_V$ over V also includes integration over a higher mass continuum with masses beyond ρ^o,ω,Φ, which at $q^2 = 0$ contributes about 22 o/o (γ_V = photon vector meson coupling, e.g. $\gamma_\rho^2/4\pi = 0.64$, m_V vector meson mass). If (1) holds, and if the photon laboratory energy ν is high enough such that

$$\frac{(m_V^2 + q^2)}{\nu} \ell_V << 1 \qquad (2)$$

(ℓ_V = mean free path of the vector meson V in nuclear matter) strong shadowing i.e. $\sigma^{\gamma A}/A\sigma^{\gamma N} < 1$, is expected [4-9] and has been observed [11] in photoproduction at energies above 4 or 5 GeV ($\sigma^{\gamma N}$ = cross section for production from nucleons N, A = mass number of the nucleus).

Due to the appearance of the propagator squared $1/(1 + q^2/m^2)^2$ in the sumrule (1), in generalized vector dominance with increasing q^2 the contribution of the smaller masses like $m_{\rho,\omega}$ to the forward virtual Compton amplitude decreases rapidly: The ρ,ω contribution in (1) drops from 73 o/o at $q^2 = 0$ to 30 o/o only at $q^2 = 1$ already, or in other words, the effective vector state mass contributing to the forward Compton amplitude increases dramatically with increasing q^2. According to (2), shadowing is then shifted to much higher energies ν. For example, for $m_V = 2m_\rho$, which is not far above the onset of the vector state continuum [1], we obtain for ν four times the value relevant in photoproduction and thus $\nu \gtrsim 20$ GeV. This qualitative argument thus already tells us that with increasing q^2 at fixed energy (say below 20 GeV), i.e. with decreasing $\omega \equiv 2M\nu/q^2$, we will find a rather rapid reduction of shadowing. Shadowing is expected to come back, however, for arbitrary fixed q^2 as soon as ν is sufficiently large for (2) to be fulfilled again.

Due to the difficulties in directly measuring the presumably multipion final state appearing in the production of higher mass ($m \gtrsim 2$ GeV) photonlike states, for $q^2 > 0$ measurements of shadowing at sufficiently high energies may be even more important as a test of sum rule (1) than it has been the case in the past for $q^2 = 0$, where ρ^o,ω,ϕ almost saturate (1).

The present paper is devoted to a quantitative analysis of the influence of higher mass vector states on shadowing in complex nuclei with emphasis on virtual photons, $q^2 > 0$. For the higher mass contributions we use the spectrum, which in ref. 1 has been shown to give a good account of deep inelastic scattering from nucleons, and it is the main aim of this paper to point out and stimulate additional experimental tests of this interpretation of the deep inelastic data.

2. Higher Mass Contributions to Shadowing

For the quantitative analysis of the influence on shadowing of higher mass photonlike states we shall treat the nucleus in a simplified manner as a sphere of constant density with radius $R = r_o A^{1/3}$ (r_o = 1.3 Fermi), A being the mass number of the nucleus. A more refined treatment of the nucleus does not seem essential at the present time due to our limited knowledge on cross section and phase for scattering of higher mass contributions on nucleons. Also, we shall concentrate on heavy nuclei, for which an optical model approach is sufficiently accurate.

2.1 A Series of Vector Mesons

Shadowing comes about through interference of the socalled one step and two step contributions to the forward Compton amplitude (Fig. 1). To order e^2, and treating the vector meson wave function in the eikonal approximation, in following e.g. the work of Brodsky and Pumplin [6], we obtain[+++]

$$\sigma_T^{\gamma A}(\nu,q^2) = A\sigma_T^{\gamma N}(W,q^2) \cdot$$

$$\left(1 - \frac{\sum_V \mathrm{Im}\frac{U_{\gamma V}^2}{(m_V^2+q^2+U_{VV})}}{\mathrm{Im}\, U_{\gamma\gamma}} + \frac{\sum_V \mathrm{Im}\left(G(X_V)\frac{U_{\gamma V}^2}{(m_V^2+q^2+U_{VV})}\right)}{\mathrm{Im}\, U_{\gamma\gamma}}\right). \qquad (3)$$

In standard notation, $\sigma_T^{\gamma N}(\sigma_T^{\gamma A})$ denotes the total hadron production cross section by transverse virtual photons of laboratory energy ν and four momentum squared q^2 on nucleons (nuclei). The sum over V runs over all vector mesons with masses m_V, which can be produced with the available photon energy ν ($\nu = (W^2-M^2+q^2)/2M$). U_{VV} is the optical potential and is related to the forward scattering amplitude of transverse vector mesons on nucleon. It may be expressed in the form

$$U_{VV}(W) = -\,\mathrm{id}\,|\vec{k}_V|\,\sigma_{VN}(W)\,(1 - i\eta_V(W)), \qquad (4)$$

where d is the nuclear density, $\vec{k}_V$ the three momentum of the vector meson V produced from a nucleon within the nucleus, σ_{VN} the transverse vector meson nucleon total cross section and η_V the ratio of the real to imaginary part of

the transverse vector meson nucleon forward scattering amplitude. Quite similarly, we have

$$\mathrm{Im}\, U_{\gamma\gamma}(W,q^2) = - d\, |\vec{q}|\, \sigma_T^{\gamma N}(W,q^2). \tag{5}$$

Finally for $U_{\gamma V}$, which is related to the vector meson forward production amplitude, we write with vector dominance

$$U_{\gamma V}(W,q^2) = \frac{\sqrt{\alpha\pi}}{\gamma_V} \frac{1}{(1+\frac{q^2}{m_V^2})} U_{VV}(W) e^{-\frac{a_V}{2}\left|t_{min}^{\gamma N \to VN}\right|}. \tag{6}$$

Here we have made use of the "diagonal approximation"[1], i.e. we neglected terms $V'N \to VN$ with $V' \neq V$. At sufficiently high energy we have $t_{min} \to 0$, and the exponential factor in (6) may be neglected. $G(X_V)$ in (3) is given by

$$G(X_V) \equiv \frac{3}{X_V^3} \left(e^{-X_V}(1 + X_V) - 1 + \frac{1}{2} X_V^2\right) \tag{7}$$

with

$$X_V = 2iR\left(|\vec{q}| - |\vec{k}_V| + \frac{1}{2|\vec{k}_V|} U_{VV}\right). \tag{8}$$

From (3) to (6) it is clear that the first two terms in (3) are volume terms proportional to A, whereas the third term due to the expressions for $G(X_V)$ and X_V contains nonlinear terms in A. For very large A the $A^{2/3}$ term is the leading one. As is well known, and can be read off from (3) and (4) easily, for sufficiently high energy such that (2) is fulfilled ($l_V \equiv 1/d\sigma_{VN}$), the volume term in (3) drops out and shadowing develops, provided

$$\sum_V \mathrm{Im} \frac{U_{\gamma V}^2}{U_{VV}} = \mathrm{Im}\, U_{\gamma\gamma} \tag{9}$$

i.e. sum rule (1) is fulfilled.

2.2 A Continuum of Vector States

In the work [1] on inelastic electron nucleon scattering by Sakurai and the present author the contribution of higher mass states (beyond ρ^o, ω, ϕ) to the virtual forward Compton amplitude (Fig. 2) has been described by a continuous spectral weight function, which we now wish to incorporate into the above formalism. For inelastic electron nucleon scattering we wrote[1] ++++ for σ_T in the diagonal approximation

$$\sigma_T^{\gamma P}(W^2,q^2) = \int \frac{\rho_T(W^2,m^2)\ m^4}{(q^2+m^2)^2}\, dm^2, \tag{10}$$

where $\rho_T(W^2,m^2)$ is related to the colliding e^+e^- beam cross section $\sigma_{e^+e^-}(m^2)$ and the vector state nucleon cross section $\sigma_{HN}(W^2,m^2)$ by

$$\rho_T(W^2,m^2) = \frac{1}{4\pi^2\alpha}\ \sigma_{e^+e^-}(m^2)\ \sigma_{HN}(W^2,m^2). \tag{11}$$

ρ_T contains a discrete and a continuum part and from ref. 1 is given by +++++

$$\rho_T(W^2,m^2) = \left[\sum_{\rho^o,\omega,\phi} r_V \delta\,(m^2-m_V^2) + r_C\ \frac{m_o^2}{m^4}\ \Theta(m^2-m_o^2)\right]\sigma^{\gamma P} \tag{12}$$

where r_V and r_C are real constants, giving percentage contributions of ρ^o,ω,ϕ and continuum to the total photoproduction cross section from protons $\sigma^{\gamma P}$, and $m_o = 1.4$ GeV is the onset of the continuum. The numerical values of r_V and r_C will be quoted below. For $W^2 \gg q^2$, i.e. ω' large, $\sigma_T^{\gamma P}$ is approximately saturated by integrating over the set of vector states only which can be actually produced at the energy considered:

$$\sigma_T(W^2,q^2) \tilde{=} \int^{(W-M)^2} \frac{\rho_T(W^2,m^2)m^4\ dm^2}{(q^2+m^2)^2}\ . \tag{13}$$

(13) is easily derived from (10) and (12): In order to make the contribution of virtual high mass vector states to the continuum part σ_T^{cont} of σ_T, $\Delta\sigma_T$, smaller ε, we must have

$$\frac{\Delta\sigma_T}{\sigma_T^{cont.}} = \frac{m_o^2+q^2}{((W-M)^2+q^2)} < \varepsilon, \tag{14}$$

and thus ω' or ω large (with $W \gg M, m_o$). Quantitatively

$$\omega' > \frac{1}{\varepsilon} \tag{15}$$

has to hold in order to fulfill (14).

In terms of the spectral weight function ρ_T we can write instead of (6)

$$\frac{d\, U^2_{\gamma V}}{dm^2}(W^2,q^2,m^2) = -d^2\,\vec{k}^2(m^2)\;\rho_T(W^2,m^2)\;\sigma_{HN}\;(W^2,m^2)\cdot$$
$$\cdot(1-i\eta_T(W^2,m^2))^2\cdot\frac{1}{(1+\frac{q^2}{m^2})^2}\,e^{-a(m^2)\left|t_{min}(W^2,q^2,m^2)\right|}. \tag{16}$$

Substituting the discrete vector meson terms appearing in (12), with (24) we recover $U^2_{\gamma V}$ of (6) upon integration over m^2. $U_{VV}(W^2,m^2)$ is now given by

$$U_{VV}(W^2,m^2) = -\,id\left|\vec{k}(m^2)\right|\;\sigma_{HN}(W^2,m^2)(1-i\eta\;(W^2,m^2)), \tag{17}$$

where as in (16) we have always indicated the dependence on the mass m of the vector state. With (13) we obtain for $\sigma_T^{\gamma A}$ the continuum generalization of (3)

$$\sigma_T^{\gamma A}(\nu,\,q^2) = A\sigma_T^{\gamma N}(W^2,q^2)\cdot$$
$$\cdot\Bigg[1-\frac{1}{\mathrm{Im}\;U_{\gamma\gamma}}\int^{(W-M)^2}\mathrm{Im}\left(\frac{dU^2_{\gamma V}}{dm^2}\;\frac{1}{(q^2+m^2+U_{VV}}\right)dm^2$$
$$+\frac{1}{\mathrm{Im}\;U_{\gamma\gamma}}\int^{(W-M)^2}\mathrm{Im}\;\left(G(X(m^2))\frac{\frac{dU^2_{\gamma V}}{dm^2}}{(q^2+m^2+U_{VV})}\right)dm^2\Bigg]. \tag{18}$$

As long as ω is large, for $m^2 \ll W^2$ we again have

$$\frac{(q^2+m^2)}{\nu}\,\ell(m^2) \ll 1 \tag{19}$$

assuming $\ell(m^2) \cong \ell_\rho$ the mean free path for ρ^o mesons. If m^2 is near the upper limit in (13), eq. (19) is not fulfilled, but this region of integration does not contribute very much to the integral, so that the second term in (18) is approximately equal to

$$\int^{(W-M)^2} \mathrm{Im}\, \frac{\frac{dU_{\gamma V}^2}{dm^2}\, dm^2}{U_{VV}} \simeq - \, d\, |\vec{q}| \int^{(W-M)^2} \frac{\rho_T(W^2,m^2)\, dm^2}{(1+\frac{q^2}{m^2})^2} \,. \tag{20}$$

From GVD, i.e. eq. (10) or rather (13) with (5) the right hand side in (20) is equal to Im $U_{\gamma\gamma}$ and shadowing again is expected to develop (for ω or ω' large).

2.3 Numerical Evaluation

For the numerical evaluation of (18) we now have to substitute the expressions (16) and (17) for $dU_{\gamma V}^2/dm^2$ and U_{VV} and also $U_{\gamma\gamma}$ from (5) and (10). The spectral weight function ρ_T appearing in (16) and (10) is given by (12) with the various contributions determined from photoproduction to be [1)]

$$\begin{aligned} r_\rho &= 0.65, \\ r_\omega &= 0.08, \\ r_\phi &= 0.05, \\ r_C &= 0.22, \end{aligned} \tag{21}$$

and

$$\sigma^{\gamma P} = (98.7 + 64.9/\sqrt{\nu})\,\mu b (\nu \text{ im GeV}). \tag{22}$$

We also note the expression for σ_T obtained upon substitution of ρ_T into (10)

$$\sigma_T^{\gamma P}(W^2,q^2) = \Big(\sum_{\rho,\omega,\phi} \frac{r_V}{(1+\frac{q^2}{m_V^2})^2} + \frac{r_C}{(1+\frac{q^2}{m_o^2})}\Big)\, \sigma^{\gamma P}. \tag{23}$$

$\sigma_T^{\gamma P}$ gives an excellent representation of the proton data in the large ω region[1)].

σ_{VN} also enters (16) and (17) directly. For V = ρ^o,ω and ϕ in consistency with (23) and the data on production from complex nuclei [++++++]

$$\sigma_{VN} = \left(\frac{\alpha\pi}{\gamma_V^2}\right)^{-1} r_V \, \sigma^{\gamma P} \tag{24}$$

with the storage ring coupling constants [13]

$$\begin{aligned} \frac{\gamma_\rho^2}{4\pi} &= 0.64 \pm 0.06 \\ \frac{\gamma_\omega^2}{4\pi} &= 4.6 \pm 0.5 \\ \frac{\gamma_\phi^2}{4\pi} &= 2.9 \pm 0.2. \end{aligned} \tag{25}$$

For $\sigma_{HN}(m^2)$ in the continuum region we shall assume

$$\sigma_{HN}(m^2) = \sigma_{\rho N}, \tag{26}$$

which from (11) and $\rho_T \sim \frac{1}{m^4}$ from (12) gives $\sigma_{e^+e^-} \sim 1/s^2$, if s denotes the e^+e^- center of mass energy. Occasionally we shall also discuss the modifications resulting from the different assumption

$$\sigma_{HN}(m^2) = \frac{m_o^2}{m^2} \sigma_{\rho N}, \tag{27}$$

in which case $\sigma_{e^+e^-} \sim 1/s$. (27) should not be taken too literally, however, particularly at very large values of m^2, as it would predict a vanishing cross section. For η, the ratio of the real to imaginary part in vector meson production, in the case of ρ^o,ω,ϕ we use $\eta = -0.2$, which is consistent with measurements [14] from the leptonic decay of photoproduced ρ^o mesons. For the continuum we shall take $\eta = 0$ and occasionally discuss the results obtained from $\eta = -0.2$. The t_{min} effect in (16) is neglected in our numerical evaluation.

The numerical evaluation then consists in adding up the ρ^o,ω,ϕ terms and integrating numerically over the continuum, as indicated more explicitly in the following formula:

$$\sigma_T^{\gamma A}(\nu,q^2) = A\,\sigma_T^{\gamma P} \cdot$$

$$\cdot\left[1 - \frac{1}{\mathrm{Im}\,U_{\gamma\gamma}}\left(\sum_{\rho^o,\omega,\phi} \mathrm{Im}\,\frac{U_{\gamma V}^2}{(q^2+m_V^2+U_{VV})} + \int_{m_o^2}^{(W-M)^2} \mathrm{Im}\left(\frac{dU_{VV}^2}{dm^2}\,\frac{1}{(q^2+m^2+U_{VV})}\right)dm^2\right)\right. \qquad (28)$$

$$+\frac{1}{\mathrm{Im}\,U_{\gamma\gamma}}\left(\sum_{\rho^o,\omega,\phi} \mathrm{Im}\,(G(X_V)\,\frac{U_{\gamma V}^2}{(q^2+m_V^2+U_{VV})}\right) +$$

$$\left. +\int_{m_o^2}^{(W-M)^2} \mathrm{Im}\,(G(X(m^2))\,\frac{dU_{\gamma V}}{dm^2}\,\frac{1}{(q^2+m^2+U_{VV})})\,dm^2\right].$$

3. Discussion of the Results

The result for $\sigma_T^{\gamma A}/A\sigma_T^{\gamma N}$ abtained for A = 207 by adding ρ^o,ω,ϕ contributions and continuum ($\eta_{cont.} = 0$) as specified above is shown in Fig. 3 as a function of ν with q^2 as parameter. Also shown is a fictitious (unrealistic) ρ^o,ω,ϕ dominance calculation for comparison. These latter results have been obtained by assuming the unrealistic coupling $\gamma_\rho^2/4\pi = 0.5$, which yields complete saturation of the sumrule for $\sigma^{\gamma P}$ by ρ^o,ω,ϕ and, as is well known, a much stronger decrease of $\sigma_T^{\gamma P}$ with q^2 than observed experimentally. The comparison of the two curves in Fig. 3 shows the expected reduction of shadowing in GVD due to the fact that the more massive sates become increasingly important with increasing q^2, and according to (2) do not strongly contribute to shadowing as long as $\nu \lesssim 20$ GeV.

In Fig. 4 we compare the GVD predictions of Fig. 3 with the experimental data [11,15]. For $q^2 > 0$ the data indicate less shadowing than calculated, although GVD lies much closer to experiment than the old ρ^o,ω,ϕ dominance results shown in Fig. 3. Also in Fig. 4, we give a quantitative answer to the question, what part of the shadowing calculated from GVD is caused by the ρ^o,ω,ϕ contribution alone. Accordingly we have put the continuum contribtuion in (28) equal to zero, but keep the complete expression (23) for σ_T (with continuum). As expected from our previous discussion, Fig. 4 shows that below 17 GeV there is no dra-

matic difference between shadowing obtained from ρ^o,ω,ϕ alone and from ρ^o,ω,ϕ plus continuum. The ρ^o,ω,ϕ curves are of interest also in connection with the experimental data, as they constitute an upper limit for $\sigma^{\gamma A}/A\sigma^{\gamma N}$. Clearly, from Fig. 4 even ρ^o,ω,ϕ alone should yield more shadowing than indicated by the data. Let us briefly mention again the assumptions on which this last result is based. We assumed for ρ^o,ω,ϕ production in the forward direction to fall off not stronger than dictated by the ρ^o,ω,ϕ propagators, and experimental evidence [16-19] so far is consistent with this expectation.+++++++ We also assumed $\eta = -0.2$ to be independent of q^2, i.e. that with increasing q^2 the vector meson production amplitude does not rapidly change phase - which seems a rather natural assumption, however. Anything, even "antishadowing" may happen[20], if phases are allowed to change rather arbitrarily. Finally, let us remark that the curves for ρ^o,ω,ϕ shadowing only in Fig. 2 are identical to the expectation from what has been called [21] ρ^o,ω,ϕ plus short range (parton) contribution. However, we have shown them not so much as predictions from an alternative model, but rather to indicate which part of the GVD results is due to low mass contributions.

Although below 20 GeV there is no dramatic difference between the shadow due to ρ^o,ω,ϕ and the one due to ρ^o,ω,ϕ plus continuum, we expect strong differences at sufficiently high energies, as the high mass states, which are dominant for $q^2 > 1\ \mathrm{GeV}^2/c^2$ become important. The high energy predictions are shown on Fig. 5, at 100 GeV also comparing with the result obtained for the ρ^o,ω,ϕ contribution solely. Above 100 GeV strong shadowing is predicted as long as $q^2 \lesssim 2\ \mathrm{GeV}^2$, equal in magnitude roughly to the one observed for photoproduction.

The results are affected, of course, by the magnitude of the vector state nucleon cross section for the high mass contribution and by a possible real part in the production amplitude. As an example of how shadowing is affected by changing the vector state nucleon amplitude for the high mass continuum states, for $\nu = 100$ GeV in Fig. 5 we also show the curves for a cross section decreasing according to (27) instead of (26) and the affect of introducing a real part equal in magnitude to the one observed for ρ^o photoproduction, $\eta_{cont.} = -0.2$. Although the amount of shadowing expected from the higher mass contributions thus has uncertainties due to our limited knowledge on their production and scattering behaviour, the predictions obtained at $\nu = 100$ GeV from the different assumptions just mentioned for $1.0 \lesssim q^2 \lesssim 2.0$ are still clearly separated from the shadowing due to ρ,ω,ϕ alone.

The final two Figures 6 and 7 are relevant to the question of scaling. Fig. 6 shows that in very good approximation $\sigma_T^{\gamma A}/A\sigma_T^{\gamma N}$ or equivalently $\nu W_{2T}^{\gamma A}/A\ \nu W_{2T}^{\gamma N}$ for $q^2 \lesssim 5$ is a function of ω only. The structure function νW_{2T}, the transverse part of νW_2, is of course related to σ_T in the usual manner

$$\nu W_{2T}^{\gamma N} = \frac{\nu - \frac{q^2}{2M}}{4\pi^2\alpha} \frac{q^2}{(q^2+\nu^2)} \sigma_T^{\gamma N} \tag{29}$$

and analogously for the nucleus. As the average mass squared $\langle m^2 \rangle$ produced diffractively increases with q^2 for $\rho \sim 1/m^4$ and σ_{HN} = const like

$$\langle m^2 \rangle \sim \text{ const. } q^2 + \text{const}_2 \equiv C_1 q^2 + C_2,$$

the significant variable determining the onset of shadowing is ω, as (2) for $\langle m^2 \rangle$ may be rewritten in terms of ω

$$\frac{C_1'}{\omega} + \frac{C_2'}{2M\nu} << 1 \tag{30}$$

We see from Fig. 6 that $\omega \gtrsim 50$ is a good estimate to specify the strong shadowing region. Finally, Fig. 7 shows what $\sigma_T^{\gamma A}/A\sigma_T^{\gamma N}$, or equivalently $\nu W_{2T}^{\gamma A}/A\nu W_{2T}^{\gamma N}$ looks like, if plotted as function of $1/\omega$. For $1/\omega < 0.1$ the same shape is obtained for $\nu W_{2T}^{\gamma A}$, as $\nu W_2^{\gamma N}$ in GVD is roughly a constant for large ω and $q^2 > 1\ \text{GeV}^2/c^2$.

4. Summarizing and Concluding Remarks

1. The main aim of this paper has been to point out quantitatively the expectation of strong shadowing in inelastic electron or muon scattering in the 100 GeV range of energies (available at NAL) for $q^2 \lesssim 2\ \text{GeV}^2$ or $\omega \gtrsim 50$. The contribution of the low lying vector mesons ρ^o, ω, ϕ to shadowing at $q^2 \simeq 1.5\ \text{GeV}^2$ and $\nu \simeq 100$ GeV is substantially smaller than the shadow expected with inclusion of higher masses. Shadowing for these values of the kinematical variables, if found experimentally, must then be due to a large extent to the propagation of higher mass states, and its experimental verification would constitute an important step forward in verifying the generalized vector dominance framework.

2. As regards the available data on inelastic electron scattering from complex nuclei at $\nu \lesssim 17$ GeV, we saw that even ρ^o, ω, ϕ should yield a larger shadow than found experimentally. Before seriously regarding more remote possibilities (which could probably fit the data) as realized in nature, e.g. a rapid change of the ρ^o production phase with increasing q^2, further experimental work on shadowing in inelastic electron or muon scattering would be desirable. The aim should be to produce data on the q^2 dependence at fixed energy, in order to clearly see the transition from strong shadowing at $q^2 = 0$ to its vanishing for sufficiently high q^2.
3. Various refinements of the present treatment can of course be worked out along with experimental progress, as e.g. taking σ_L into account, using a more realistic nuclear model etc. We do not think, however that such refinements change our main expectation of large shadowing mainly due to higher mass vector states in the hundred GeV range for modestly large $q^2 \lesssim 2$ GeV^2 (or $\omega \gtrsim 50$).

Acknowledgement

I would like to thank Professors Sid Drell and W. Panofsky for their warm hospitality and many experimental and theoretic1 colleagues at SLAC for stimulating discussions on this subject, in particular James Bjorken, Stan Brodsky, Fred Gilman, Ted Murphy and Leo Stodolsky.

LITERATURE

1 J.J. Sakurai and D. Schildknecht,
Phys. Letters 40B (1972) 121
Phys. Letters 41B (1972) 489
Phys. Letters 42B (1972) 216

2 A. Bramón, E. Etim and M. Creco,
Phys. Letters 41B (1972) 609

3. G. Bacci et al., Phys. Letters 38B (1972) 551
G. Barbarino et al., Lettere al Nuovo Cimento 3 (1972) 689
H.H. Bingham et al., SLAC-PUB-1113 and LBL - 1085 (1972)
M. Davier et al., SLAC-PUB-666 (1969)

4. L. Stodolsky, Phys. Rev. Letters 18 (1967) 135

5. K. Gottfried and D.R. Yennie, Phys. Rev. 182 (1969) 1595

6. S. Brodsky and J. Pumplin, Phys. Rev. 182 (1969) 1794

7. M. Nauenberg, Phys. Rev. Letters 22 (1969) 556

8. B. Margolis and C.L. Tang, Nucl. Phys. B10 (1969) 329

9. V.N. Gribov, Soviet Phys. JETP 30 (1970) 709

10. P.G.O. Freund, Nuovo Cimento 44A (1966) 411
H. Joos, Phys. Letters 24B (1967) 103
K. Kajantie and J.S. Trevil, Phys. Letters 24B (1967) 1o6

11. V. Heynen et al., Phys. Letters 34B (1971) 651
D.O. Caldwell et al., UCSB preprint (1972)
G.R. Brookes et al., Daresbury report DNPL/P136 (1972)

12. K. Gottfried in Proceedings of the 1971 International Conference on Electron and Photon Interactions at High Energies, Cornell University, Ithaca N.Y. (1971)

13. J. Lefrancois, V.A. Sidorov, Proceedings of the 1971 International Conference on Electron and Photon Interactions at High Energies, Cornell University, Ithaca N.Y. (1971)

14. H. Alvensleben et al., Phys. Rev. Letters 25 (1970) 1377

15. H. Kendall, Report in Proceedings of the 1971 International Conference on Electron and Photon Interactions at High Energies, Cornell University, Ithaca N.Y. (1971)

16. C. Driver et al., Nucl. Physics B38 (1972) 1
and Erratum, to be published

17. V. Eckardt et al., DESY 72/67 (1972)

18. J.T. Dakin et al., SLAC-PUB-1154 (1972)

19. J. Ballam et al., Contribution to the 16. International Conference on High Energy Physics, Chicago and Batavia, Ill. (1972)

20. G.V. Bochmann, Phys. Rev. 6 (1972) 2715

21. S.J. Brodsky et al, Phys. Rev. D6 (1972) 177

Footnotes

+ For related work compare also ref. 2.

++ $f_{\gamma V}^{T}$ is actually to be taken at $-t = (q-k_V)^2 = 0$, which coincides with the forward direction for $W \to \infty$ only.

+++ We restrict ourselves to the transverse part of the electroproduction cross section. The change in the result for $\sigma^{\gamma A}/A\sigma^{\gamma N}$ should not be very significant, if the longitudinal part is taken into account also.

++++ The expression (10) for σ_T with (11) is, of course, nothing else but the sum rule (1) rewritten in a slightly different form.

+++++ We use the expression for inelastic scattering from protons and neglect the neutron proton difference, which is small in the region of $\omega > 10$ of interest in this paper.

++++++ See e.g. reference 12 for a recent summary.

+++++++ The result from ref. 18 for transverse ρ^o production by virtual photons especially at $q^2 = 0.7\ GeV^2/c^2$ seems somewhat low however, when compared with the ρ^o dominance prediction.

Figure Captions

Fig. 1 The one step and two step contributions to the Compton forward scattering amplitude

Fig. 2 Forward Compton scattering in the Vector Dominance Model.

Fig. 3 Prediction for $\sigma_T^{\gamma A}/A\sigma_T^{\gamma N}$ in GVD compared with an unrealistic ρ^o,ω,ϕ dominance calculation (assuming saturation of sum rule (1) by ρ^o,ω,ϕ only).

Fig. 4 Prediction for $\sigma_T^{\gamma A}/A\sigma_T^{\gamma N}$ in GVD compared with photoproduction [11] and inelastic electron scattering [15] data. Compare text for details. (The longitudinal contribution has been neglected in the theory, but is, of course included in the experimental data).

Fig. 5 Prediction from GVD for $\sigma_T^{\gamma A}/A\sigma_T^{\gamma N}$ at high energies, presently obtainable at NAL. At ν = 100 GeV we also show the change in the predictions resulting from different assumptions on the behaviour of the high mass continuum and the contribution due to ρ^o,ω,ϕ alone. Compare text for details.

Fig. 6 $\sigma_T^{\gamma A}/A\sigma_T^{\gamma N}$ as a function of ω for fixed q^2.

Fig. 7 Same as Fig. 6, but as a function of $\frac{1}{\omega}$.

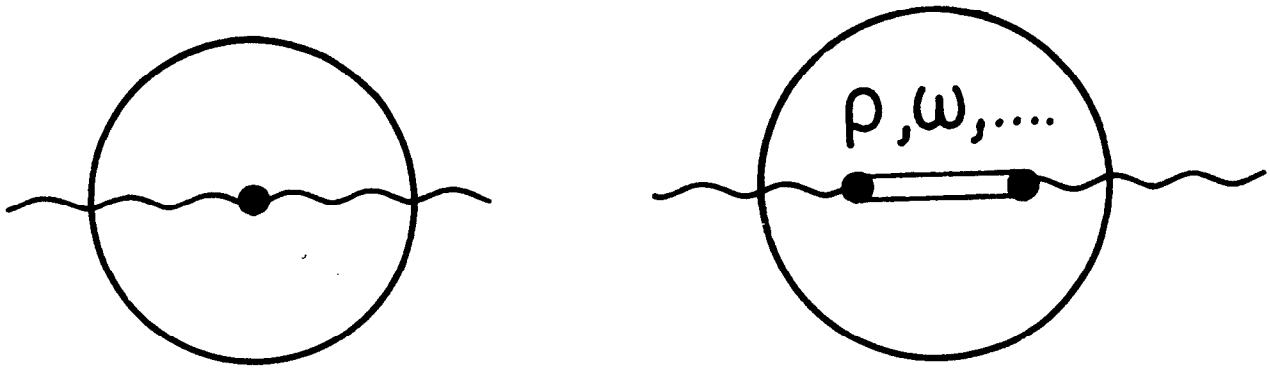

Fig.1

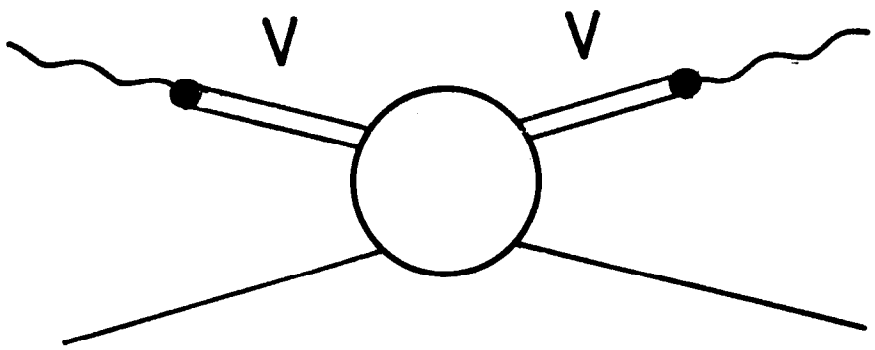

Fig.2

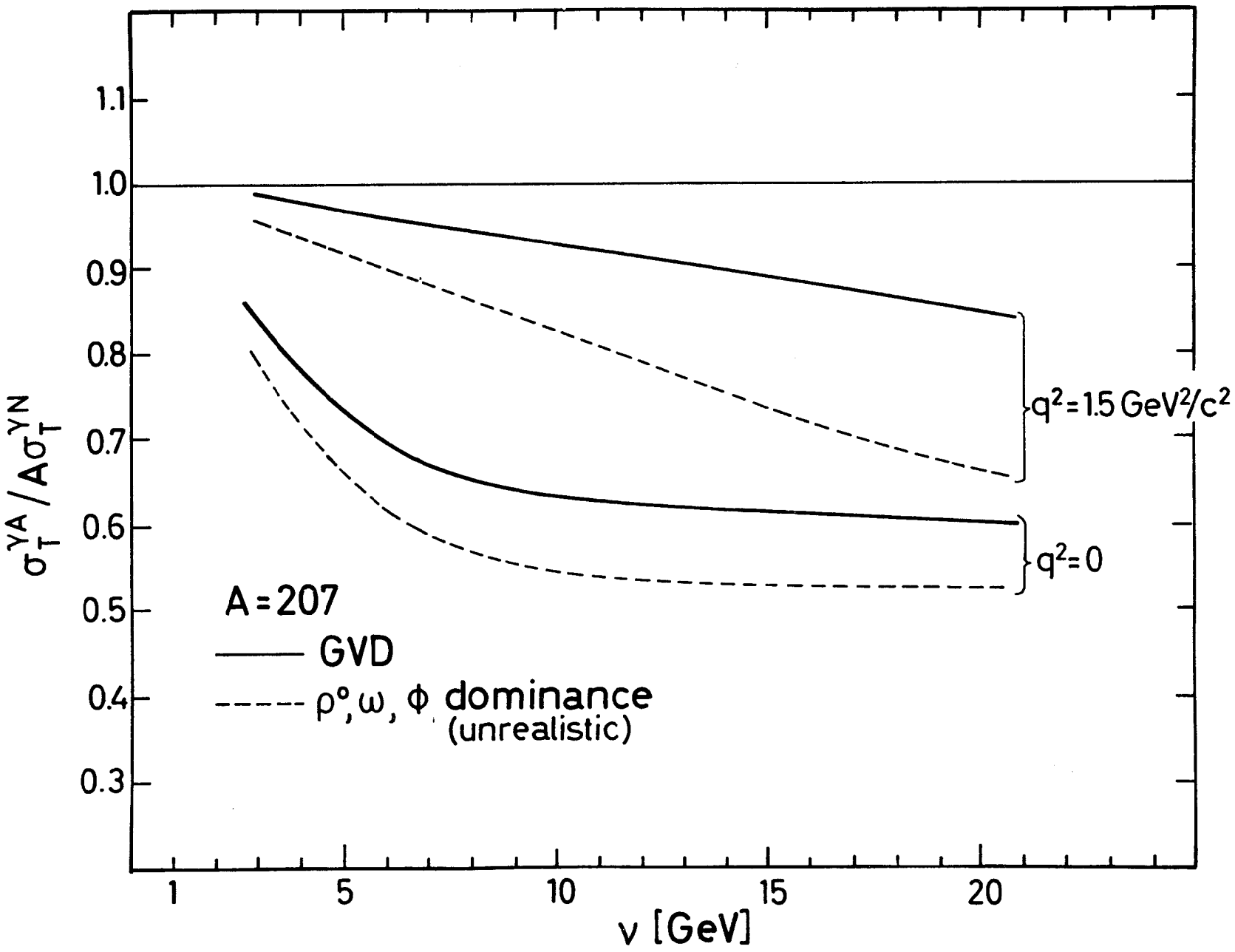
1.1
1.0
0.9
0.8
0.7
0.6
0.5
0.4
0.3
$\sigma_T^{\gamma A} / A\sigma_T^{\gamma N}$
$q^2 = 1.5\ GeV^2/c^2$
$q^2 = 0$
A = 207
GVD
ρ^o, ω, ϕ dominance
(unrealistic)
1
5
10
15
20
ν [GeV]

Fig. 3

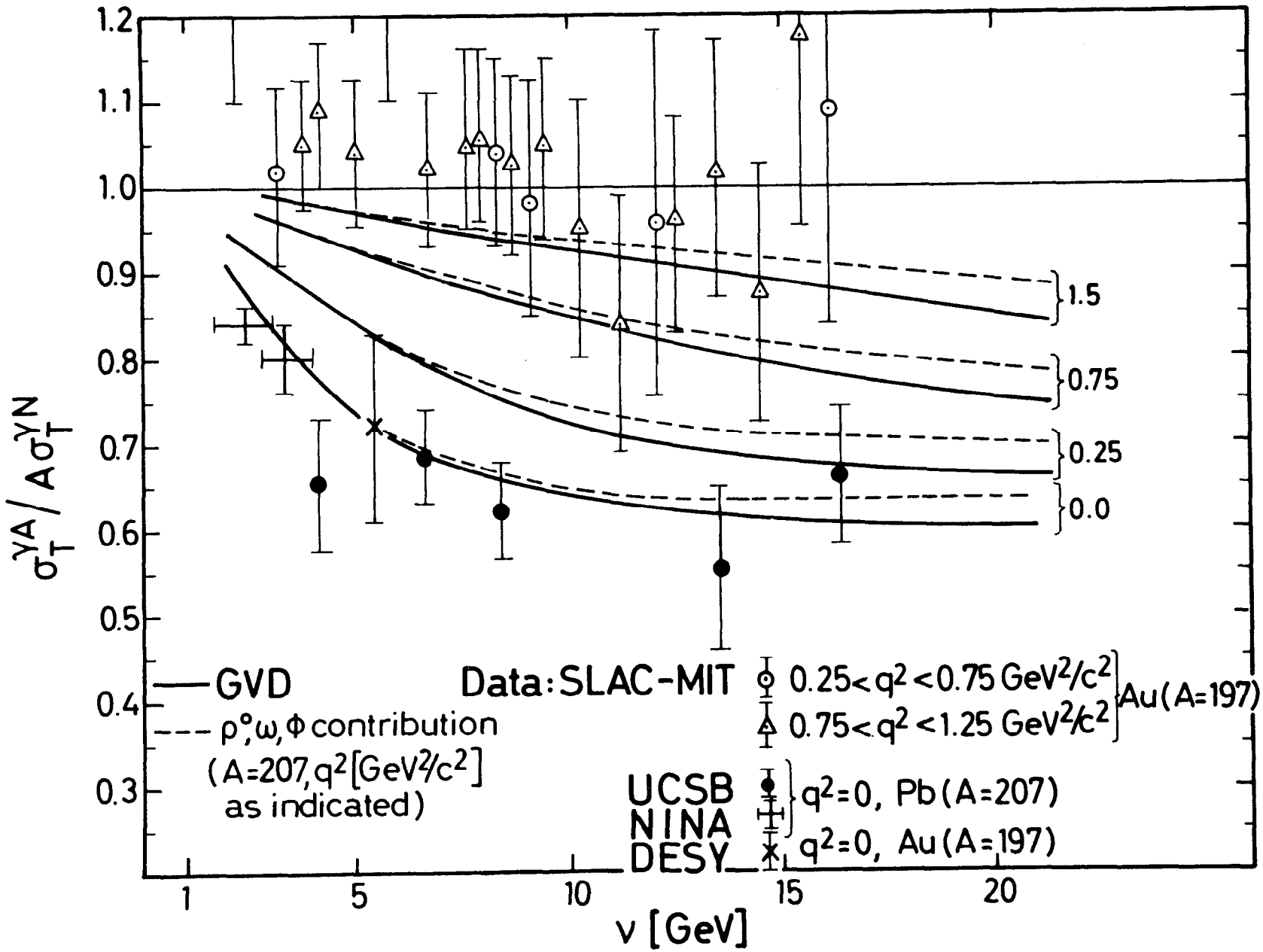
1.2
1.1
1.0
0.9
0.8
0.7
0.6
0.5
0.4
0.3
$\sigma_T^{\gamma A} / A\sigma_T^{\gamma N}$
1.5
0.75
0.25
0.0
GVD
ρ°,ω,Φ contribution
(A=207, q² [GeV²/c²] as indicated)
Data: SLAC-MIT
0.25<q²<0.75 GeV²/c²
0.75<q²<1.25 GeV²/c²
Au (A=197)
UCSB
NINA
DESY
q²=0, Pb (A=207)
q²=0, Au (A=197)
1
5
10
15
20
ν [GeV]

Fig. 4

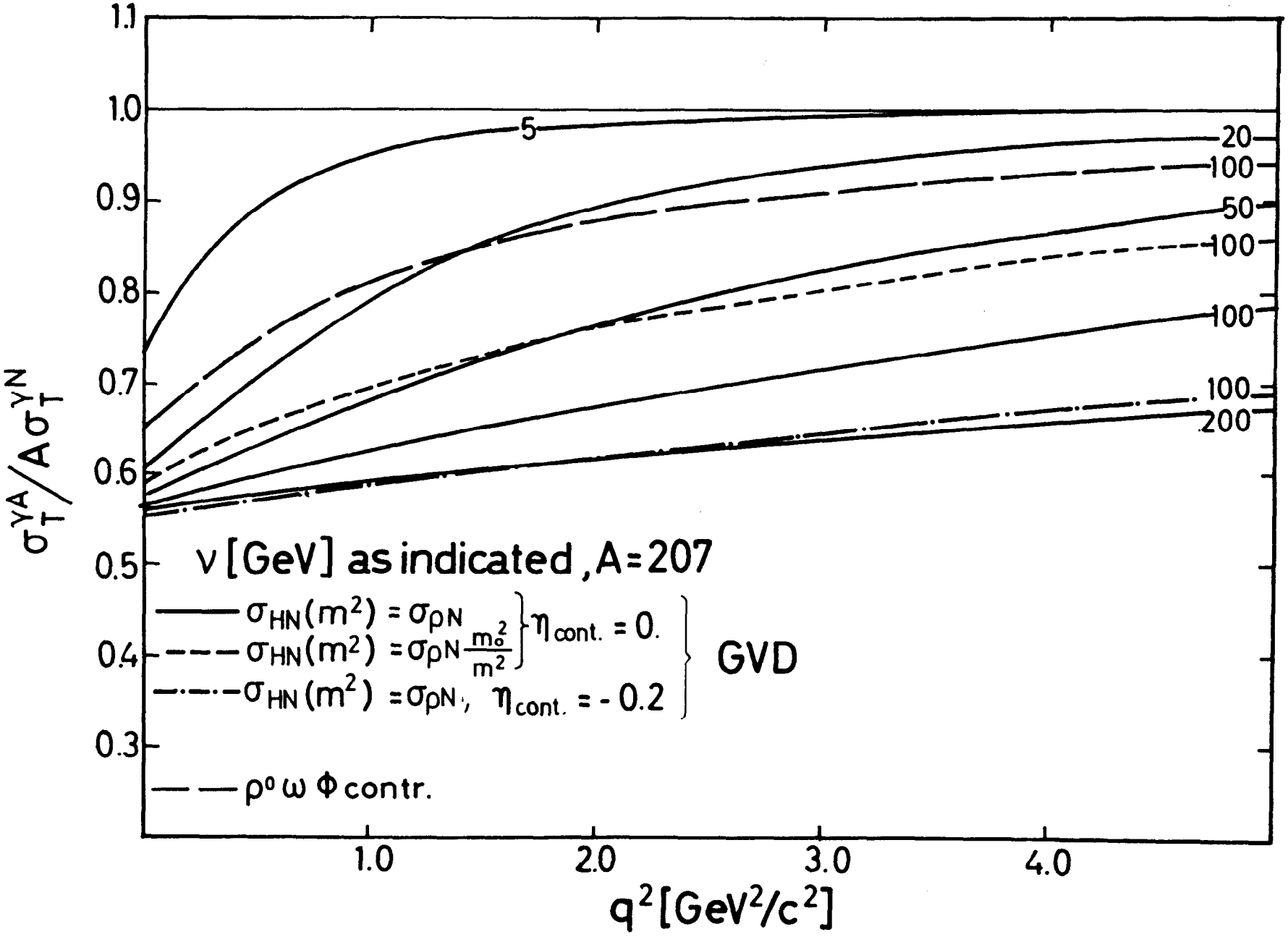
1.1
1.0
0.9
0.8
0.7
0.6
0.5
0.4
0.3
$\sigma_T^{\gamma A}/A\sigma_T^{\gamma N}$
5
20
100
50
100
100
100
200
ν [GeV] as indicated, A=207
$\sigma_{HN}(m^2) = \sigma_{\rho N}$
$\sigma_{HN}(m^2) = \sigma_{\rho N}\frac{m_o^2}{m^2}$
$\eta_{cont.} = 0.$
$\sigma_{HN}(m^2) = \sigma_{\rho N}$, $\eta_{cont.} = -0.2$
GVD
$\rho^0\,\omega\,\Phi$ contr.
1.0
2.0
3.0
4.0
q^2 [GeV^2/c^2]

Fig. 5

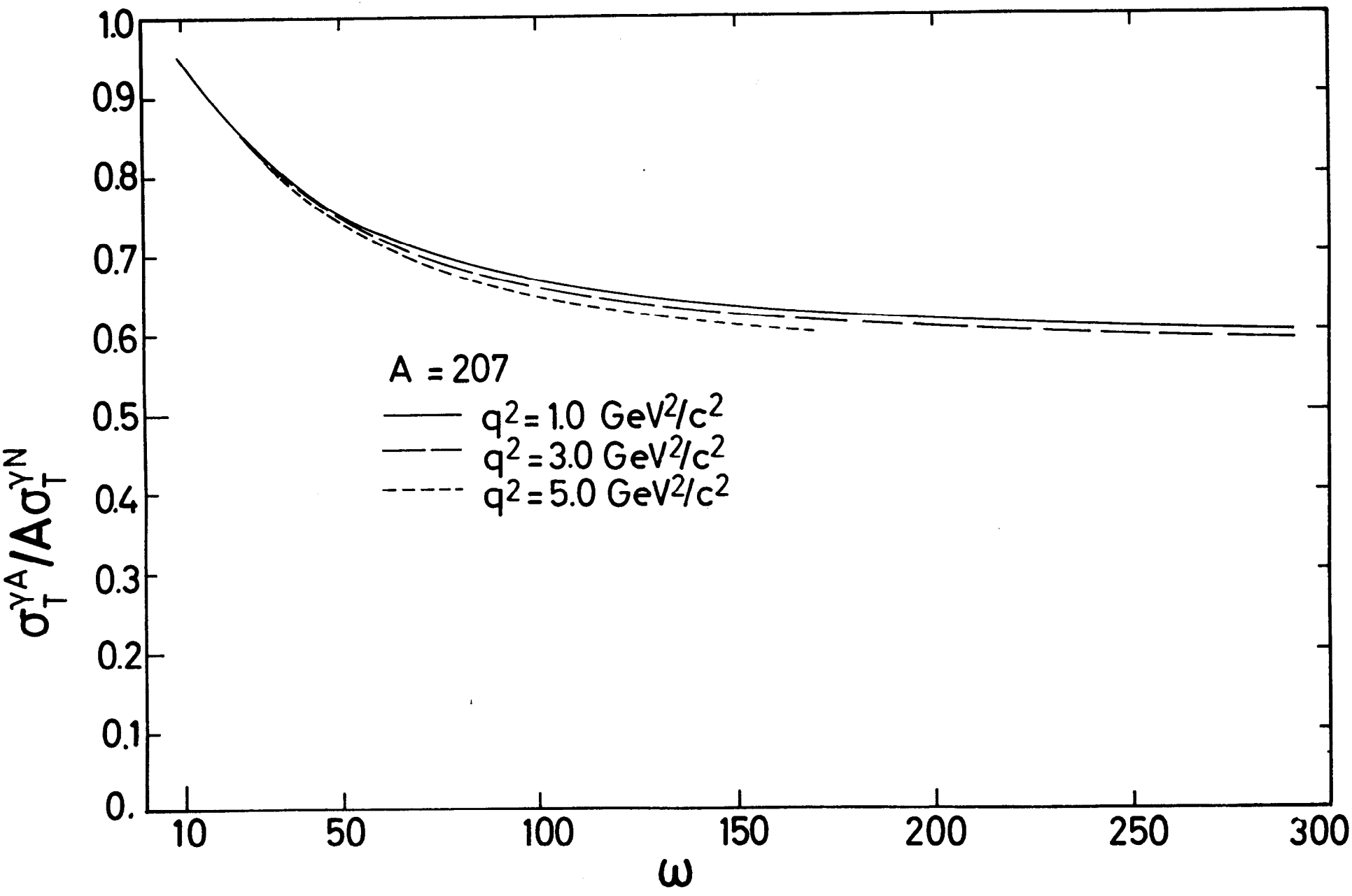
1.0
0.9
0.8
0.7
0.6
0.5
0.4
0.3
0.2
0.1
0.
10
50
100
150
200
250
300
ω
$\sigma_T^{\gamma A}/A\sigma_T^{\gamma N}$
A = 207
$q^2 = 1.0\ GeV^2/c^2$
$q^2 = 3.0\ GeV^2/c^2$
$q^2 = 5.0\ GeV^2/c^2$

Fig. 6

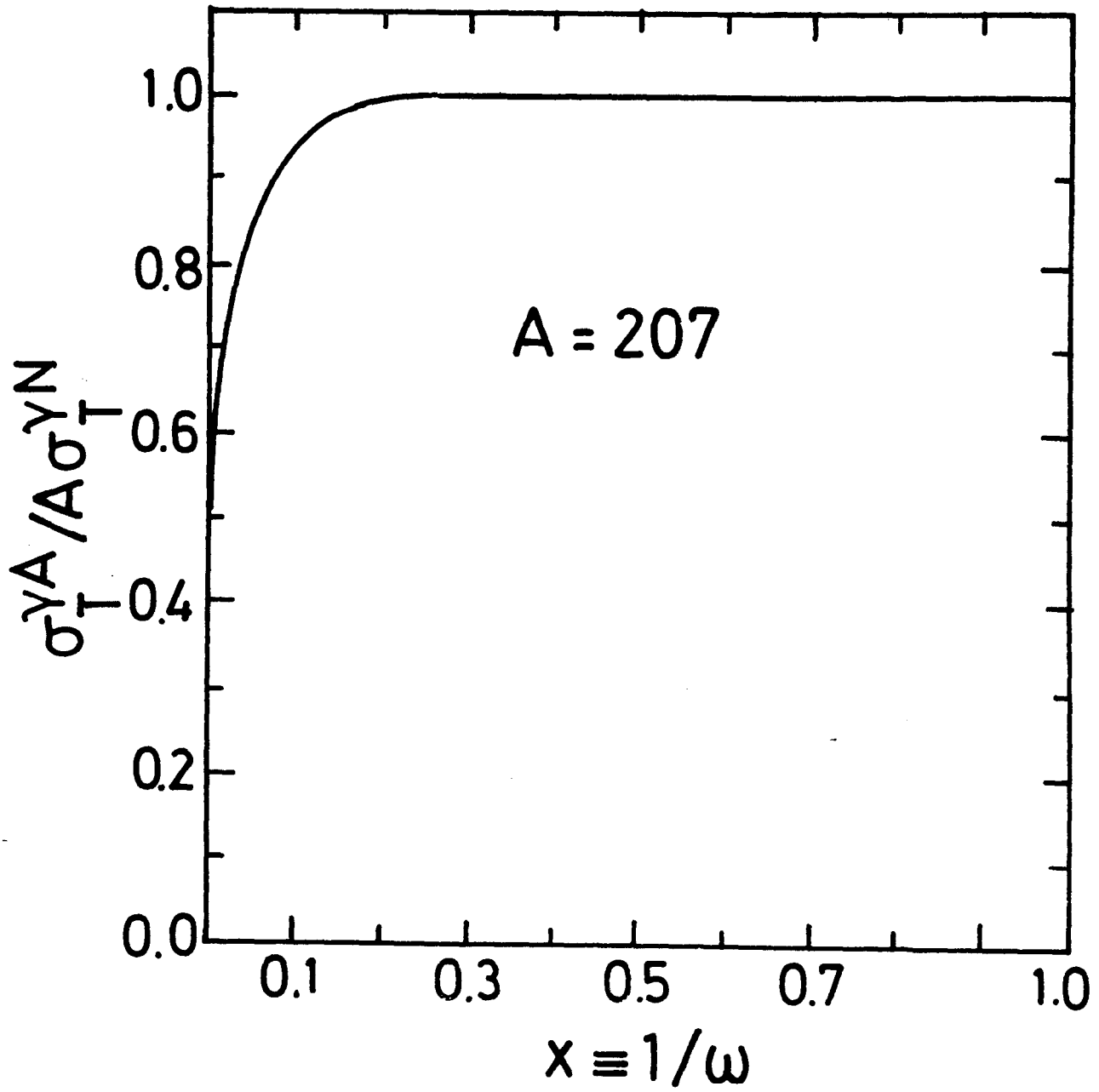
1.0
0.8
0.6
0.4
0.2
0.0
$\sigma_T^{\gamma A}/A\sigma_T^{\gamma N}$
A = 207
0.1
0.3
0.5
0.7
1.0
$x \equiv 1/\omega$

Fig. 7